Research Article | Vol. 24, No. 21 | 17 Oct 2016 | OPTICS EXPRESS 24137

Optics EXPRESS

Scattering-assisted second harmonic generation of structured fundamental wave

HAIGANG LIU,[1,2] JUN LI,[3] XIANGLING FANG,[1,2] XIAOHUI ZHAO,[1,2] YUANLIN ZHENG,[1,2,4] AND XIANFENG CHEN[1,2,5]

[1]*State Key Laboratory of Advanced Optical Communication Systems and Networks, Department of Physics and Astronomy, Shanghai Jiao Tong University, Shanghai 200240, China*
[2]*Key Laboratory for Laser plasma (Ministry of Education), Collaborative Innovation Center of IFSA (CICIFSA), Shanghai Jiao Tong University, Shanghai 200240, China*
[3]*Science and Technology College, Jiangxi Normal University, Jiangxi 330027, China*
[4]*ylzheng@sjtu.edu.cn*
[5]*xfchen@sjtu.edu.cn*

Abstract: We study a scattering-assisted second harmonic generation process of a structured fundamental wave, whose phase front is periodically modulated, in a homogenous nonlinear medium. Scattering-assisted multiple-conical second harmonic in a one-dimensional structured fundamental wave and second harmonic belts in two-dimensional cases were observed. The experimental results are consistent with our analysis. This method not only allows dynamic control of the scattering-assisted second harmonic signal, but also has potential applications in various nonlinear frequency conversion processes.

OCIS codes: (190.0190) Nonlinear optics; (050.1970) Diffractive optics; (190.2620) Harmonic generation and mixing.

References and links

1. P. Xu, S. Ji, S. Zhu, X. Yu, J. Sun, H. Wang, J. He, Y. Zhu, and N. Ming, "Conical second harmonic generation in a two-dimensional $\chi^{(2)}$ photonic crystal: A hexagonally poled $LiTaO_3$ crystal," Phys. Rev. Lett. **93**, 133904 (2004).
2. N. An, Y. Zheng, H. Ren, X. Deng, and X. Chen, "Conical second harmonic generation in one-dimension nonlinear photonic crystal," Appl. Phys. Lett. **102**, 201112 (2013).
3. H. Huang, C. Huang, C. Zhang, D. Zhu, X. Hong, J. Lu, J. Jiang, Q. Wang, and Y. Zhu, "Second-harmonic generation in a periodically poled congruent $LiTaO_3$ sample with phase-tuned nonlinear cherenkov radiation," Appl. Phys. Lett. **100**, 022905 (2012).
4. Z. Xie, G. Zhao, P. Xu, Z. Gao, and S. Zhu, "Study of optical elastic scattering in a quasiperiodically poled $LiTaO_3$ crystal," J. Appl. Phys. **101**, 056104 (2007).
5. T. Li, X. Zhao, Y. Zheng, and X. Chen, "Conical second harmonic generation in KDP crystal assisted by optical elastic scattering," Opt. Express **23**, 23827–23833 (2015).
6. P. Xu, S. Zhu, X. Yu, S. Ji, Z. Gao, G. Zhao, Y. Zhu, and N. Ming, "Experimental studies of enhanced raman scattering from a hexagonally poled $LiTaO_3$ crystal," Phys. Rev. B **72**, 064307 (2005).
7. J. Armstrong, N. Bloembergen, J. Ducuing, and P. Pershan, "Interactions between light waves in a nonlinear dielectric," Phys. Rev. **127**, 1918 (1962).
8. S. M. Saltiel, D. N. Neshev, R. Fischer, W. Krolikowski, A. Arie, and Y. S. Kivshar, "Generation of second-harmonic bessel beams by transverse phase-matching in annular periodically poled structures," Jpn. J. Appl. Phys. **47**, 6777 (2008).
9. W. Wang, Y. Sheng, Y. Kong, A. Arie, and W. Krolikowski, "Multiple čerenkov second-harmonic waves in a two-dimensional nonlinear photonic structure," Opt. Lett. **35**, 3790–3792 (2010).
10. P. Molina, M. Rami´ rez, B. Garci´ a, and L. Bausa, "Directional dependence of the second harmonic response in two-dimensional nonlinear photonic crystals," Appl. Phys. Lett. **96**, 261111 (2010).
11. Y. Sheng, D. Ma, and W. Krolikowski, "Randomized nonlinear photonic crystal for broadband optical frequency conversion," J. Phys. At. Mol. Opt. Phys. **46**, 215401 (2013).
12. Y. Sheng, W. Wang, R. Shiloh, V. Roppo, Y. Kong, A. Arie, and W. Krolikowski, "Cerenkov third-harmonic generation in $\chi^{(2)}$ nonlinear photonic crystal," Appl. Phys. Lett. **98**, 241114 (2011).
13. X. Hong, B. Yang, C. Zhang, Y. Qin, and Y. Zhu, "Nonlinear volume holography for wave-front engineering," Phys. Rev. Lett. **113**, 163902 (2014).
14. N. V. Bloch, K. Shemer, A. Shapira, R. Shiloh, I. Juwiler, and A. Arie, "Twisting light by nonlinear photonic crystals," Phys. Rev. Lett. **108**, 233902 (2012).
15. A. Shapira, R. Shiloh, I. Juwiler, and A. Arie, "Two-dimensional nonlinear beam shaping," Opt. Lett. **37**, 2136–2138 (2012).

#273893 http://dx.doi.org/10.1364/OE.24.024137
Journal © 2016 Received 15 Aug 2016; revised 29 Sep 2016; accepted 30 Sep 2016; published 10 Oct 2016

Optics EXPRESS

16. T. Ellenbogen, N. Voloch-Bloch, A. Ganany-Padowicz, and A. Arie, "Nonlinear generation and manipulation of airy beams," Nat. Photonics **3**, 395–398 (2009).
17. S. Trajtenberg-Mills, I. Juwiler, and A. Arie, "On-axis shaping of second-harmonic beams," Laser Photon. Rev. **9**, L40–L44 (2015).
18. A. Shapira, L. Naor, and A. Arie, "Nonlinear optical holograms for spatial and spectral shaping of light waves," Sci. Bull. **60**, 1403–1415 (2015).
19. A. Shapira, I. Juwiler, and A. Arie, "Nonlinear computer-generated holograms," Opt. Lett. **36**, 3015–3017 (2011).
20. Y. Zhang, J. Wen, S. Zhu, and M. Xiao, "Nonlinear talbot effect," Phys. Rev. Lett. **104**, 183901 (2010).
21. Y. Sheng, A. Best, H.-J. Butt, W. Krolikowski, A. Arie, and K. Koynov, "Three-dimensional ferroelectric domain visualization by čerenkov-type second harmonic generation," Opt. Express **18**, 16539–16545 (2010).
22. Y. Lin, K. Su, K. Huang, and Y. Chen, "Pattern formation of second harmonic conical waves in a nonlinear medium with extended defect structure," Opt. Express **22**, 27859–27868 (2014).
23. A. Libster-Hershko, S. Trajtenberg-Mills, and A. Arie, "Dynamic control of light beams in second harmonic generation," Opt. Lett. **40**, 1944–1947 (2015).
24. H. Liu, J. Li, X. Zhao, Y. Zheng, and X. Chen, "Nonlinear raman-nath second harmonic generation with structured fundamental wave," Opt. Express **24**, 15666–15671 (2016).
25. V. Roppo, K. Kalinowski, Y. Sheng, W. Krolikowski, C. Cojocaru, and J. Trull, "Unified approach to Cerenkov second harmonic generation," Opt. Express **21**, 25715-25726 (2013).

1. Introduction

Scattering phenomenon has been extensively investigated in nature. In general, scattering of light could be a detrimental effect in some fields, such as optical communication and imaging system, but it could also be beneficial in others. For instance, scattering could be used to discover structure information and physical properties of the materials relating to light-matter interaction. Not limited in linear optics, such scattering phenomenon has also been reported in processes of nonlinear frequency conversion [1–6], in which the nonlinear signal is enhanced because of the phase matching of the incident and scattered light in some special directions. The quasi-phase matching(QPM) method allows to phase match a nonlinear process in the transparency range of the nonlinear photonic crystals (NPCs) by spatially modulating its nonlinear coefficient. Since QPM proposed by Bloembergen et al. in 1962 [7], plenty of phase-matching geometries by diverse types of one- and two-dimensional NPCs, including square, hexagonal lattices, annular periodical, or even random structures [8–12] have been studied. Such special designed NPCs not only provide a method to enhance the conversion efficiency of the nonlinear signal, but also provide a platform to shape the light beam in nonlinear manner [13–19]. Moreover, the nonlinear signals also can be used to enclose the structure property of the nonlinear crystal directly. Thus it is a way to probe the structure of NPCs using optical methods [20–22]. Nevertheless, the limitations of such special structured NPCs are the complex fabrication and fixed properties. Hence, how to manipulate the nonlinear signal pattern in real time has become an urgent issue.

Considering a degenerate second harmonic generation (SHG) process, the nonlinear polarization , which serves as the source of second harmonic (SH), excited by the fundamental wave (FW) in a nonlinear medium can be expressed as $P_{2\omega}(r,t) = \epsilon_0 \chi^{(2)}(r) E_\omega^2(r,t)$, where ϵ_0 is the vacuum permittivity, $\chi^{(2)}$ is the second-order susceptibility and E_ω is the electric field of FW. It indicates that the SHG not only relates to $\chi^{(2)}$, but also the structure of the incident FW. This makes it possible to manipulate the SH pattern in real time by controlling the incident FW [23–25].

In this paper we studied scattering-assisted SHG process of structured FW, whose phase front is periodically modulated. When transverse phase periodical modulated FW propagates along a homogenous second order nonlinear medium, scattering-assisted multiple-conical SH can be observed. This method provides a way to manipulate the scattering-assisted SH signal in real time and has potential applications in various nonlinear frequency conversion processes.

Optics EXPRESS

2. The theoretical analysis

In order to study such scattering-assisted conical SH and without loss of generality, a 5-mol%MgO:$LiNbO_3$ bulk crystal ($10 \times 1 \times 10$ mm^3 dimensions) is used to provide an anomalous-dispersion-like condition ($2k_{1,o} > k_{2,e}$) at room temperature. The incident light and scattered light can be expressed as: $\vec{E}_1 = A_1 exp[-i(\vec{k}_1 \cdot \vec{r} - \omega t)]$, $\vec{E}_1^{'} = A_1^{'} exp[-i(\vec{k}_1^{'} \cdot \vec{r} - \omega t)]$, where A_1 , $\vec{k}_1$ and $A_1^{'}$, $\vec{k}_1^{'}$ are amplitudes and wave vectors of the incident and scattered light, respectively. When the wavefront is phase modulated, the incident light can be written as an expansion of Fourier series:

$$\vec{E}_1 = A_1 \cdot \sum C_m exp(-i\vec{G}_m \cdot \vec{r}) exp[-i(\vec{k}_{ym} \cdot \vec{r} - \omega t)] \tag{1}$$

where C_m and $G_m = 2\pi m/\Lambda$ are the Fourier coefficients and reciprocal vectors of the FW, Λ is the period of the FW modulation. $\vec{G}_m$ is perpendicular to $\vec{k}_{ym}$ since only the transverse phase is modulated. The relation between G_m and k_{ym} are $G_m^2 + k_{ym}^2 = k_1^2$. The incident light and the scattered light stimulate a sum frequency polarization wave, which can be expressed as:

$$\vec{P}_2 = \epsilon_0 \chi^{(2)} \vec{E}_1 \vec{E}_1^{'} = \epsilon_0 \chi^{(2)} A_1 A_1^{'} \sum C_m exp[-i(\vec{k}_{ym} + \vec{k}_1^{'} + \vec{G}_m) \cdot \vec{r} + i2\omega t)] \tag{2}$$

Therefore the phase-matching condition of scattering-assisted conical SHG can be written as $\vec{k}_{ym} + \vec{k}_1^{'} + \vec{G}_m = \vec{k}_2$, where $\vec{k}_2$ is wave vector of SH beam. If the phase of incident FW period is sharply modulated from 0 to ϕ and the duty cycle D is 0.5. The Fourier coefficients can be derived as

$$C_0 = \frac{1}{2}(1 + e^{i\phi}), \; C_m = \frac{i[\cos(m\pi) - 1]}{2m\pi}(1 - e^{i\phi}) \tag{3}$$

Note that the Fourier coefficients C_m are non-zero only for odd values of m (except C_0). The scattering-assisted conical SH intensity is proportional to the C_m, and can be expressed as $I_2 = |C_m|^2 \left|\chi^{(2)}\right|^2 I_1 I_1^{'}$. Where I_1, $I_1^{'}$ and I_2 are the intensities of the incident light, the scattered FW, and their corresponding SHG, respectively.

3. Experiment results and discussion

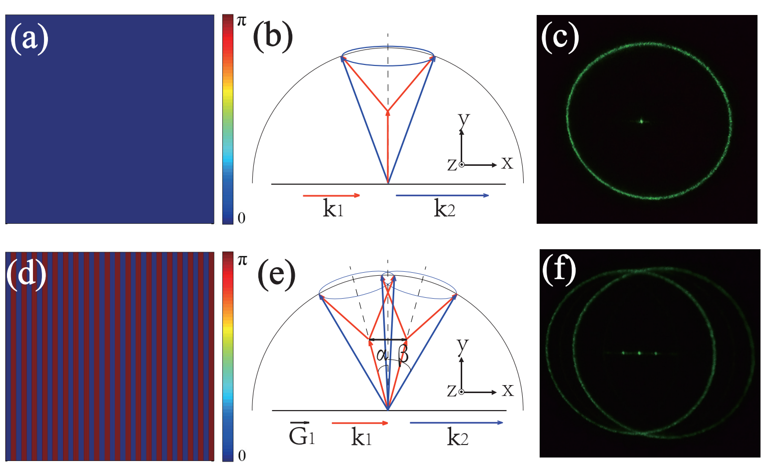

Fig. 1. (a)(d) The phase structure of the FW. (b)(e) Phase-matching geometries of scattering-assisted conical SHG process with different structure of FW corresponding to (a)(d), respectively. (c)(f) Observed SH patterns in experiment corresponding to (a)(d), respectively.

In our experiment, the FW at a wavelength of 1064 nm (Nd:YAG nanosecond laser) was phase modulated by a spatial light modulator (SLM). The SLM had a resolution of 512 × 512 pixels, each with a rectangular area of 19.5 × 19.5 μm^2. The FW was then imaged by a 4-f system (magnification of 0.25) to imprint the modulated wavefront pattern to the onset of a $\chi^{(2)}$ crystal. The beam waist was reduced to 2 mm. The FW was kept as o-polarized and propagated along the y-axis of the crystal at room temperature. After the crystal, a shortpass filter was used to filter out the FW. Finally, the generated SH beam was projected on a screen in the far-field and recorded by a camera.

In order to illustrate the role of structured FW, we did a compared experiment without phase structure of the FW, see Figs. 1(a)-1(c). The type of SH interaction is $e_2 - o_1 o_1$. Then, the phase of FW is period sharply modulated from 0 to π in 1D structure. The phase structure of the FW is illustrated in Fig. 1(d), which exhibits 1:1 duty cycle. In this situation, the Fourier coefficients become $C_0 = 0$ and $C_m = \frac{-2i}{m\pi}[\sin(\frac{m\pi}{2})]^2$. The scattering-assisted conical SH intensity can be express as $I_2 = I_1 I_1' \left|\chi^{(2)}\right|^2 [\frac{2}{m\pi}\sin(\frac{m\pi}{2})]^2$, which is the same as the conical SH intensity in PPLN [2]. A set of symmetrically distributed ring-shaped SH, in which 0, ±1 and ±3 orders of SH ring in experiment, observed, as shown in Fig. 1(f). In principle, only odd order SH rings exist and the intensity is proportional to $|C_m|^2$. In fact, 0 order SH ring with a low intensity observed in experiment comes from the imperfect structure of FW. Higher order SH rings are not observed owing to the smaller Fourier coefficients.

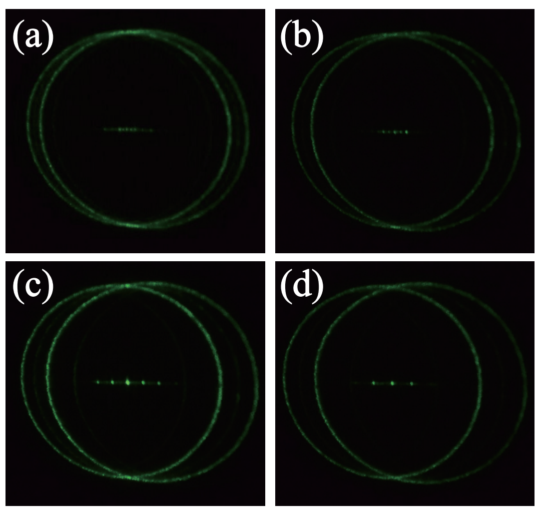

Fig. 2. Photos of SH evolving with periods of the FW. (a-d) 125 μm, 83.3 μm, 62.5 μm and 50 μm, respectively.

The evolution of SH varying with periods of FW is shown in Fig. 2. The period of the FW are 125, 83.3, 62.5 and 50 μm, respectively, corresponding to Figs. 2(a)-2(d). With decreasing of FW period, the two scattering SH ring separates in space and the distance is increasing.

To accurately describe the position of scattering-assisted conical SH, parameters α and β are introduced and depicted in Fig. 1(e). Theoretical expression of the parameters can be described in the following form:

$$\alpha = arc\sin\left(\frac{\vec{G}_m}{\left|\vec{k}_{1,o}\right|}\right),\ \beta = arc\cos\left(\frac{\left|\vec{k}_{2,e}\right|}{2\left|\vec{k}_{1,o}\right|}\right) + \alpha \tag{4}$$

The optical periods (50, 55.6, 62.5, 71.4, 83.3, 96.2, 125, 166.7 and 250 μm) were varied to measure α and β, as illustrated in Fig. 3(a), which is consistent with the theoretical calculation.

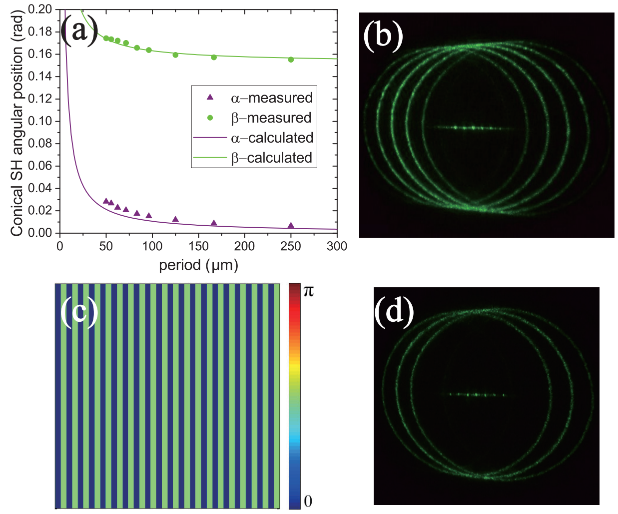

Fig. 3. (a) Angles α and β as a function of the FW period. Theoretical prediction (solid curves) and measured ones (signs) are in well agreement with each other. (b) SHG in case of FW periodic modulated from 0 to π and D=0.6. (c) FW periodic modulated from 0 to $\pi/2$ in 1D structure. (d) SHG corresponding to (c).

A more general case of periodic 1D modulation occurs when the duty cycle is not 0.5. The Fourier coefficients can be expressed as $C_0 = 2D - 1$, $C_m = \frac{2\sin(m\pi D)}{m\pi}$. In this case, each order of C_m is non-zero. Therefore, in experiment, the 0, ±1 and ±2 order scattering-assisted SH ring can be observed, as in Fig. 3(b) with D=0.6.

According to the analysis, scattering-assisted conical SHG with phase period sharply modulated from 0 to π exhibits similar results in PPLN analyzed in [2]. In fact, in PPLN, the simulated nonlinear polarized wave experiences an opposite phase in the two adjacent opposite domains, which is caused by the sharp modulation from +1 to −1. When the phase of FW is period sharply modulated from 0 to π along the transverse direction in a bulk medium, it excites similar nonlinear polarization wave. So it is straightforward to imagine that it will exhibit similar phenomenon in the process of SHG as that in 1D NPCs. However, there still exists some difference between these two schemes. In PPLN, the reciprocal vector of the QPM grating compensates for the wavevector mismatch between the FW and SH. But the reciprocal vector provided by the structured FW only leads to the diffraction of the FW.

Secondly, from the Fourier coefficient of Eq. (3), the value of ϕ determine the existence of C_0 and the relative value of C_m (the value of C_m are still 0 for the even values of m). The structure of FW is illustrated in Fig. 3(c) in the case of FW modulated from 0 to $\pi/2$ in 1D structure with 1:1 duty cycle. The multiple-conical SHG is depicted in Fig. 3(d) in which 0, ±1 and ±3 orders can be observed.

Furthermore, interesting phenomena happen with the phase of FW period sharply modulated from 0 to π in 2D structure. The annular phase structure of the FW is illustrated in Fig. 4(a) in which $D = 0.5$ and the period corresponds to 50 μm. The phase-matching geometry with radial direction reciprocal vectors is shown in Fig. 4(b). Instead of multiple ring in 1D structure of FW, the overlapping area of ±1 order rings of conical SH forms a belt region of SH [depicted in Fig. 4(c)] because of cylindrical symmetry. The inner region of the SH belt is brighter than the outer edge caused by higher SH density. There still exists SH between the center and ±1 order SH belt, which are caused by the overlapping of ±3 order conical SH ring (±3 order SH belt).

Optics EXPRESS

As a matter of fact, the area of ±3 order SH belt is larger than ±1 order SH belt, however, only inner region of the ±3 order SH belt is observed in Fig. 4(c) because of lower SH density. In the discussed case of $LiNbO_3$ (and most nonlinear crystals, which are negative uniaxial ones), the scattering-assisted conical SH only can be realized in the anomalous-dispersion-like condition ($2k_{1,o} > k_{2,e}$). And such an anomalous-dispersion-like condition could not be satisfied along z direction in an ambient environment. Therefore, such scattering-assisted conical SH could not be observed in the annually poled ferroelectric crystal.

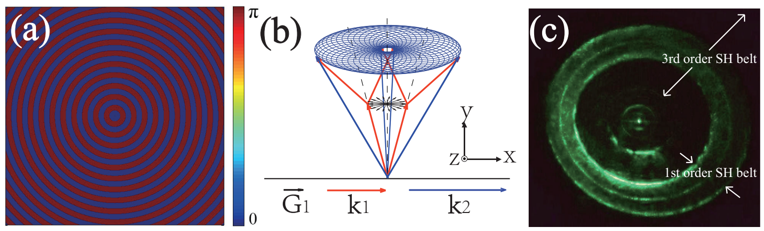

Fig. 4. (a) The annular phase structure of the FW. (b) Phase-matching geometries of scattering-assisted conical SHG process with annular structure of FW. (c) Observed SH belts in experiment.

The phase modulation of the FW itself for nonlinear wave mixing features many advantages. Actually, compared to $\chi^{(2)}$ modulation, it is more flexible to modulate the FW itself [23, 24]. Firstly, this method does not require special sample fabrication procedures. Secondly, the FW can be controlled by an SLM in real time, whereas SHG in NPCs is fundamentally restricted by their predesigned structures. Moreover, the modulated FW can propagate along any direction of bulk nonlinear medium. This is important for efficient SHG by utilizing larger components of the $\chi^{(2)}$ tensor. Although the advantages of the wavefront modulation with respect to the spatial material modulation are quite obvious, there are also some drawbacks. The SLM device cannot handle with highly intense laser beams, which high conversion efficient nonlinear processes depend on. The minimum period of the structured FW is limited by the pixel size of the SLM, which in turn limits the angle of the SH radiation. These are the tradeoffs that need to be considered and coped with in experiments and future potential applications. Although the same experimental set-up is used in [24], different nonlinear processes are studied in the work in [23,24] and in this paper. The work in [23] deals with on-axis shaping the SH beam, while work in [24] deals with off-axis nonlinear Raman-Nath diffraction. In this paper, scattering-assisted second harmonic generation process of structured fundamental wave is carefully studied.

4. Conclusion

In conclusion, we studied scattering-assisted SHG process of structured FW, whose phase front is periodically modulated. In the case of 1D structure of FW, the multiple-conical SH was observed and the position measured in experiments was consistent with theoretical analysis. Extending such structured FW to 2D case, scattering-assisted SH belts were also observed in experiments. This method not only allows dynamic control of the scattering-assisted SH signal, but also has potential applications in various nonlinear frequency conversion processes, such as nonlinear Raman-Nath diffraction, nonlinear Bragg diffraction and nonlinear Cerenkov radiation, etc.

Funding

National Natural Science Foundation of China (NSFC) (61125503, 61235009, 11421064); The Foundation Development of Science and Technology of Shanghai (13JC1408300).